Polarized Raman Study of Aligned Multiwalled Carbon Nanotubes

A. M. Rao*

Center for Applied Energy Research, Department of Physics and Astronomy, University of Kentucky, Lexington, Kentucky 40506

A. Jorio, M. A. Pimenta, and M. S. S. Dantas

Departamento de Fisica, Universidade Federal de Minas Gerais, Belo Horizonte, 30123-970 Brazil

R. Saito

Department of Electronics-Engineering, University of Electro-Communications, Tokyo, 182-8585 Japan

G. Dresselhaus and M. S. Dresselhaus

Massachusetts Institute of Technology, Cambridge, Massachusetts 02139-4307

(Received 15 September 1999)

Polarized Raman spectra of high purity aligned arrays of multiwalled carbon nanotubes, prepared on silica substrates from the thermal decomposition of a ferrocene-xylene mixture, show a strong dependence of the graphitelike G band and the disorder-induced D band on the polarization geometry employed in the experiments. The experimental G-band intensity exhibits a minimum at $\theta_m = 55°$ in the VV configuration, in good agreement with theoretical predictions of a characteristic minimum at 54.7° for A_{1g} modes in single wall nanotubes, where θ_m denotes the angle between the polarization direction and the nanotube axis.

Aligned multiwalled carbon nanotubes (MWNTs) are of interest for both fundamental and applied carbon research [1,2]. The fundamental structural anisotropy of carbon nanotubes, due to their high aspect ratio (length/diameter), suggests the importance of polarized Raman spectroscopy studies. The high structural anisotropy results in quasicontinuous wave vectors along the nanotube axis and discrete wave vectors in the circumferential direction, giving rise to anisotropy in the electrical, optical, and magnetic properties. For example, de Heer *et al.* [3] prepared aligned MWNTs by an imprinting technique to determine the anisotropic dielectric properties along the directions parallel and perpendicular to the nanotube axis. The practical realization of efficient electron emission from aligned MWNT arrays has opened possibilities for using aligned nanotubes as novel tiny electron guns for flat screen displays [4].

Much effort has been devoted to prepare aligned nanotube arrays using preformed substrates. Based on the catalytic decomposition of a ferrocene-xylene mixture (Fe ~ 0.75 at.%) near atmospheric pressure at ~ 700 °C, Andrews *et al.* [5] recently described a simple, inexpensive method for producing bulk quantities of high purity MWNTs, with an average nanotube diameter $d_t \sim 25$ nm, and aligned normal to bare silica substrates. In this Letter, we use polarized Raman spectroscopy on aligned MWNTs prepared by this method [5] to compare the observed graphitelike G-band polarization intensities and their angular dependence with theoretical predictions for single wall nanotubes (SWNTs) and to show that the observed relative intensities of the Raman D band ($1320-1400$ cm^{-1} in Fig. 1) and G band

($1530-1640$ cm^{-1}) are sensitive to the orientation of the optical electric field with respect to the nanotube axis.

Sun *et al.* [6] previously studied the polarized Raman spectra of SWNTs synthesized in the porous channels of aluminophosphate single crystals, observing radial and tangential G bands at ~ 530 cm^{-1} and ~ 1600 cm^{-1}, respectively, indicating nanotube diameters of <5 Å [7]. Their study finds that the intensity of the tangential Raman band is sensitive to the polarization geometry, with the tangential mode intensity being the strongest for the incident and scattered optical E fields along the tube axis in agreement with our results, as discussed below. Using a Lorentzian line shape analysis, their tangential band was resolved into three modes at 1585 (E_{2g}; 36), 1599 (E_{1g}; 56), and 1615 (A_{1g}; 30) cm^{-1}, where the first entry in the parentheses corresponds to the assigned symmetry label and the second entry represents the full width at half maximum (FWHM) linewidth. In contrast to the results of Sun *et al.* [6], we conclude that the A_{1g}, E_{1g}, and E_{2g} tangential mode frequencies for our multiwall nanotube sample have a spread of ~ 5 cm^{-1}.

Polarized Raman experiments in the vicinity of the D and G bands were performed on aligned MWNTs at room temperature using a DILOR XY micro-Raman spectrometer and 514.5 nm laser excitation. The thickness of the aligned bundle was intentionally kept below 1 μm so that the focused laser excitation beam (diameter ~ 1 μm) overfilled the aligned bundle of MWNTs during all polarized Raman scattering measurements.

The inset in Fig. 1 schematically represents a MWNT bundle oriented along the x direction. Also shown in Fig. 1 are Raman spectra for the various directions x and y used
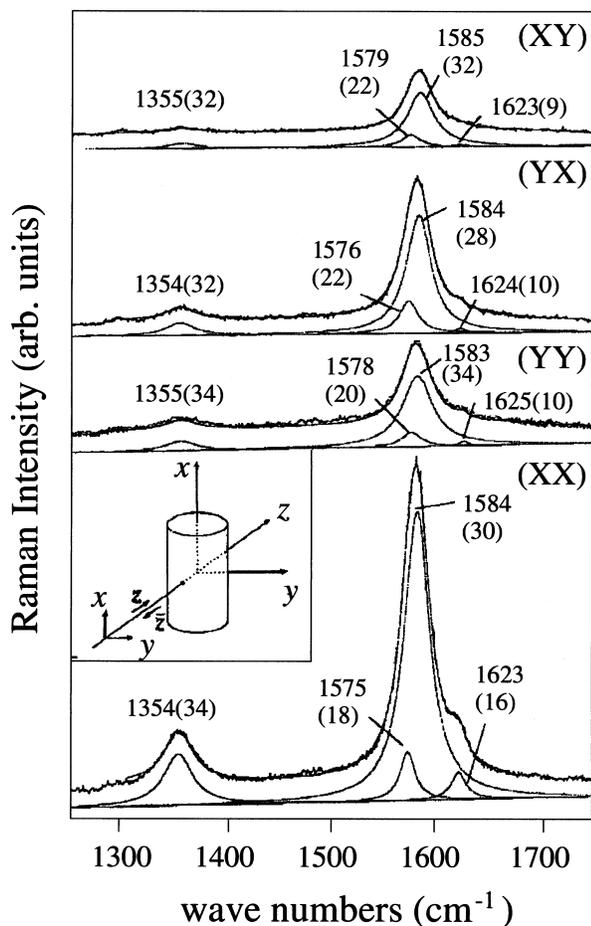
FIG. 1. Polarized Raman spectra for MWNTs taken at 514.5 nm (2.41 eV) for four scattering geometries, showing peak frequencies for the various features (full width half maximum FWHM linewidths in parentheses). The inset defines the polarization geometries for the aligned nanotubes that lie parallel to the x axis.

for the polarization directions X and Y of the incident and scattered light, which form the focus of this paper. It can be seen that the intensities of the D and G bands are sensitive to the scattering geometries with the greatest intensities observed for the (XX) polarization geometry. The usual notation for a backscattering Raman experiment is $Z(XY)\overline{Z}$ to indicate light incident along the Z axis with electric vector in the X direction and scattered light along the $-Z$ direction with electric vector in the Y direction. Since all our experiments are carried out in the backscattering geometry with light normal to the nanotube axis, we use the abbreviated notation giving only the incident and scattered electric field directions. The observed polarization dependence suggests that the observation of the D band in the Raman spectrum of MWNTs (where the D band is generally associated with the presence of disorder or finite size effects in sp^2 carbons) does not necessarily imply that the MWNTs have a disordered wall structure. Further support for this conclusion comes from comparing the polarized (XX) and (XY) Raman spectra of MWNTs in
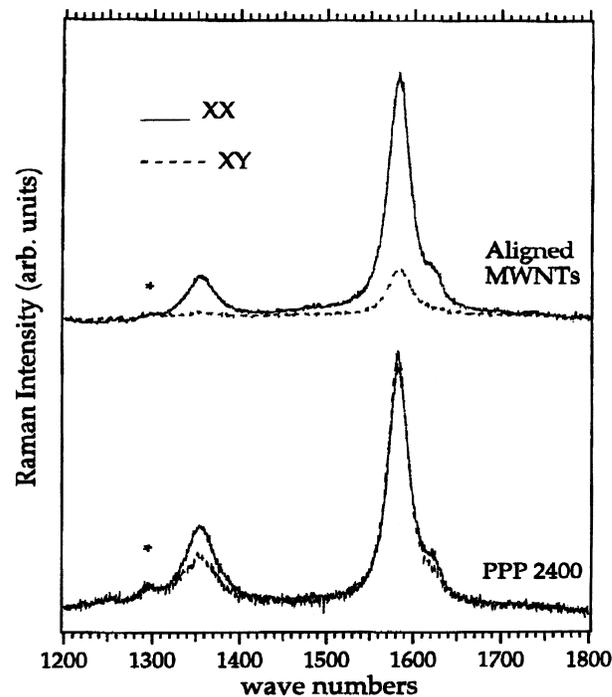
FIG. 2. Polarized Raman spectra with (XX) and (XY) polarization geometries from an sp^2 turbostratic carbon sample of PPP-2400, polyparaphenylene heat treated to 2400 °C, in comparison to the corresponding spectra for MWNTs. The peaks indicated by an "*" are a Raman microscope artifact.

Fig. 2 with the corresponding spectra obtained from an sp^2 turbostratic disordered carbon sample of PPP-2400 under experimental conditions similar to those used in Fig. 1. The comparison shows that the relative integrated intensities of the D and G bands for the MWNTs depend strongly on polarization, while the dependence of the PPP-2400 spectra shows only a dependence of the *disorder-induced* features at about 1355 and 1620 cm^{-1} on the polarization geometry. It is significant that the D-band polarization dependence for the MWNTs and for the PPP-2400 samples are different.

A Lorentzian line shape analysis for the MWNTs spectra in Fig. 1 shows four peaks at 1355, 1576, 1584, and 1624 cm^{-1} in almost all the polarization geometries, but with very different polarization-dependent relative intensities, as summarized in Table I. We therefore conclude that all four features are intrinsic to the MWNTs. From Fig. 1, the experimental polarized G-band integrated intensity ratios are $XX{:}YY{:}XY{:}YX = 1.00{:}0.29{:}0.19{:}0.39$ for our MWNTs.

TABLE 1. Summary of experimental polarization results.

Geometry	I_{1355}/I_{1583}	I_{1576}/I_{1583}	I_{1624}/I_{1583}
(XY)	0.083	0.137	0.024
(YX)	0.121	0.206	0.015
(YY)	0.134	0.122	0.016
(XX)	0.204	0.098	0.053

First we comment on the three principal frequencies associated with the G band in Fig. 1. The nanotube geometry results in slightly different force constants along the nanotube axis relative to the circumferential direction, where the nanotube curvature reduces the force constant. This anisotropy in the force constant accounts for the frequency difference between the components at 1575 cm^{-1} (attributed to vibrations in the circumferential direction) and at 1584 cm^{-1} (attributed to vibrations along the nanotube axis) for the (XX) polarization. Similar splittings are observed for the other polarization geometries, and all splittings averaged to 1580.8 ± 0.8 cm^{-1}, in good agreement with the E_{2g_2} graphite mode frequency. Because of the small number of allowed k vectors in the circumferential direction, we expect this frequency difference to increase with decreasing nanotube diameter [8], so that SWNTs with diameters of $d_t \sim 1.4$ nm show a mode splitting [9] of 1567 and 1593 cm^{-1}, which also averages to ~ 1580 cm^{-1}. The feature near 1620 cm^{-1} which is quite pronounced in the spectra for MWNTs and not present in SWNTs is associated with the maximum in the graphene 2D phonon density of states [2].

No theory has yet been developed to describe polarization effects for MWNTs. Therefore we apply the theory developed for (10,10) SWNTs [10] as a first approximation for interpreting the experimental results obtained for the G-band intensities in Fig. 1 for MWNTs. The theory of polarization effects in single wall nanotubes should allow us to distinguish between contributions to the G band from tangential modes with A_{1g}, E_{1g}, and E_{2g} symmetry [10], which according to bond polarization model calculations [10,11] for a (10,10) SWNT predict Raman-active frequencies at 1587, 1585, and 1591 cm^{-1}, respectively, all occurring within a range of 6 cm^{-1}, which is smaller than the observed G-band linewidth for Raman scattering [6,10].

The polarization geometries used in the theoretical intensity calculations [10] (see inset in Fig. 1) are expressed in terms of the angle θ_m between the nanotube axis and the polarization direction. The intensities for the (XX) and (YY) geometries correspond, respectively, to $\theta_m = 0$ and $\theta_m = 90°$ for the VV polarization configuration, while the (XY) and (YX) geometries, respectively, correspond to $\theta_m = 0$ and $\theta_m = 90°$ for the VH configuration, where V and H denote vertical and horizontal, respectively. In the (XX) configuration, the A_{1g} mode is dominant for the tangential band, while in the (YY) configuration, both the A_{1g} and E_{2g} modes contribute to the scattering intensity. The intensity ratios predicted for the A_{1g} mode at $\theta_m = 0$, the A_{1g} mode at $\theta_m = 90°$, and the E_{2g} mode at $\theta_m = 90°$ are, respectively, 2.91, 0.72, and 0.33 [10]. Thus the theoretical value for the intensity ratio for (XX) and (YY) is $2.91/1.05 = 1.00/0.36$, which is to be compared to the experimental values of 1.00/0.29.

Calculations for the expected Raman intensity for the (XY) and (YX) geometries show an angular dependence for a rotation of the nanotube around its own axis (θ_3 in

Ref. [10]). Thus by taking an average of the E_{1g} mode intensity over θ_3, we get a theoretical value for the intensity ratio for the (XY) to (YX) geometries of $0.300/0.081 = 1.00/0.27$, which is to be compared with the experimental value of 0.49/1.00.

In summary, the theoretical predictions for the G-band relative intensities for SWNTs are 1.00:0.36:0.13:0.03 for the $(XX):(YY):(XY):(YX)$ polarization geometries, to be compared with the corresponding experimental values for aligned MWNTs, 1.00:0.29:0.19:0.39. In principle, the Raman frequencies associated with the XX, XY, and YX polarizations for SWNTs should give the frequencies for mode symmetries A_{1g}, E_{1g}, and $(E_{1g} + E_{2g})$, respectively. Our measurements indicate that the mode frequencies for these three modes lie within ~ 5 cm^{-1} and are unresolved within the G-band linewidth.

Theoretically, the intensity of the tangential A_{1g} mode is expected to exhibit a minimum at $\theta_m = \cos^{-1}(1/\sqrt{3}) = 54.7°$ [10]. Figure 3 shows a collection of Raman spectra that were obtained on aligned MWNTs in the VV configuration as a function of θ_m. Clearly the experimental G-band intensity exhibits a characteristic minimum
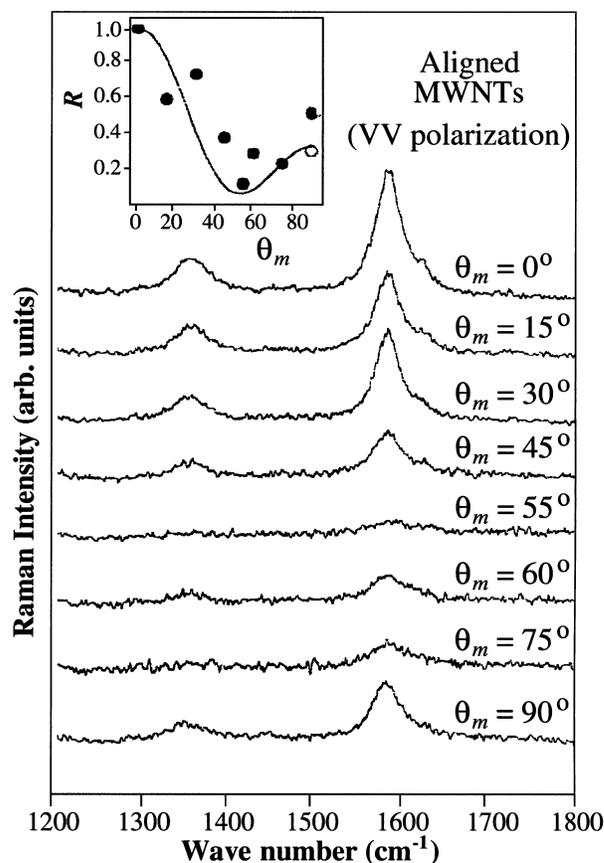
FIG. 3. Dependence of the Raman intensity for VV scattering as a function of the measured angle θ_m between the polarization direction and the nanotube axis (see inset in Fig. 1). The inset to this figure shows the dependence of the experimental G-band intensity ratio R (open and filled circles) as a function of θ_m in comparison to theory for SWNTs (see text) [10].

near $\theta_m = 55°$, in excellent agreement with the theory developed for SWNTs. The inset in Fig. 3 shows good overall agreement between theory and experiment for the G-band intensity ratio (R) at θ_m compared to the corresponding intensity at $\theta_m = 0°$. It should be noted that the intensity ratio R denoted by the open circle in the inset in Fig. 3 was obtained from the XX and YY data depicted in Fig. 1. The data set in Fig. 3 also suggests that the G-band intensity is dominated by the intensity of the A_{1g} symmetry mode at 1584 cm^{-1}. It is interesting that the D-band intensity is also a minimum near $\theta_m = 55°$.

It would also be interesting to measure polarization effects associated with the A_{1g} *radial breathing mode* in SWNTs. Since the A and B carbon atoms within the unit cell of the graphene 2D honeycomb lattice move similarly under breathing mode displacements, there should be no intensity for the (XY) or (YX) polarization geometries in isolated SWNTs. Theory for SWNTs further predicts that the (YY) intensity should be stronger than that for the (XX) intensity, with a polarization intensity ratio (XX):(YY) = 0.20:1.00 for the radial breathing mode, if we neglect the depolarization effect of carbon nanotubes discussed below. Since the intensity of the radial breathing mode drops rapidly with increasing tube diameter [where we note that the intensity of this mode for a (20,20) tube is vanishingly small [12]], polarization studies of the radial breathing mode should be done on SWNTs with $d_t < 1.5$ nm.

Returning to Fig. 1 we note that the optical absorption spectra of a single wall carbon nanotube, calculated for polarized light by Ajiki and Ando [13,14], show that the selection rule for optical absorption between the valence and conduction π subbands with subband index n is $\Delta n = 0$ and $\Delta n = 1$ for polarization parallel and perpendicular to the nanotube axis, respectively. They show that the optical absorption for the polarization perpendicular to the nanotube axis is suppressed almost completely when the depolarization effect is taken into account. Thus the optical absorption occurs only when the polarization is parallel to the nanotube axis for intersubband transitions, with $\Delta n = 0$ for single wall carbon nanotubes. The depolarization effect should, however, be relaxed in MWNTs, especially as the diameter increases. On the basis of the depolarization effect, we expect more effective excitation of resonant Raman scattering for the (XX) scattering geometry, and for metallic nanotubes, for which the nanotube acts as a radiation pipe for the laser excitation. The polarized Raman spectra for aligned MWNTs in Fig. 1 appear to be consistent with the optical anisotropy present in the MWNTs, and the discrepancy between the experimental polarized Raman intensity ratios and theoretical predictions may be due to a depolarization (antenna) effect which tends to enhance the experimental YX:XY intensity ratio.

In explaining the D-band frequency shifts with laser excitation energy it was noted that the mechanism giving rise to the D-band vibrations involves carbon atom vibrations with A_{1g} symmetry on every other hexagonal ring on a $\sqrt{3} \times \sqrt{3}$ superlattice [15]. Because of these symmetry-related phenomena, it is of interest to study the polarization effects associated with the D band both experimentally and theoretically.

*Corresponding author.
Email address: rao@pop.uky.edu

[1] M. S. Dresselhaus, G. Dresselhaus, and P. C. Eklund, *Science of Fullerenes and Carbon Nanotubes* (Academic Press, New York, 1996).

[2] R. Saito, G. Dresselhaus, and M. S. Dresselhaus, *Physical Properties of Carbon Nanotubes* (Imperial College Press, London, 1998).

[3] W. A. de Heer, A. Châtelain, and D. Ugarte, Science **270**, 1179 (1995).

[4] Y. Saito, S. Uemura, and K. Hamaguchi, Jpn. J. Appl. Phys. **37**, L346 (1998).

[5] R. Andrews, D. Jacques, A. M. Rao, F. Derbyshire, D. Qian, X. Fan, and E. C. Dickey, Chem. Phys. Lett. **303**, 467 (1999).

[6] H. D. Sun, Z. K. Tang, J. Chen, and G. Li, Solid State Commun. **109**, 365 (1999).

[7] S. Bandow, S. Asaka, Y. Saito, A. M. Rao, L. Grigorian, E. Richter, and P. C. Eklund, Phys. Rev. Lett. **80**, 3779 (1998).

[8] A. Kasuya, Y. Sasaki, Y. Saito, K. Tohji, and Y. Nishina, Phys. Rev. Lett. **78**, 4434 (1997).

[9] A. M. Rao, E. Richter, S. Bandow, B. Chase, P. C. Eklund, K. W. Williams, M. Menon, K. R. Subbaswamy, A. Thess, R. E. Smalley, G. Dresselhaus, and M. S. Dresselhaus, Science **275**, 187 (1997).

[10] R. Saito, T. Takeya, T. Kimura, G. Dresselhaus, and M. S. Dresselhaus, Phys. Rev. B **57**, 4145 (1998).

[11] R. Saito, T. Takeya, T. Kimura, G. Dresselhaus, and M. S. Dresselhaus, Phys. Rev. B **59**, 2388 (1999).

[12] S. L. Fang, A. M. Rao, P. C. Eklund, P. Nikolaev, A. G. Rinzler, and R. E. Smalley, J. Mater. Res. **13**, 2405 (1998).

[13] H. Ajiki and T. Ando, Physica (Amsterdam) **201B**, 349 (1994).

[14] H. Ajiki and T. Ando, Jpn. J. Appl. Phys. Suppl. **34-1**, 107 (1995).

[15] M. J. Matthews, M. A. Pimenta, G. Dresselhaus, M. S. Dresselhaus, and M. Endo, Phys. Rev. B **59**, R6585 (1999).